Lattice QCD Evidence that the $\Lambda(1405)$ Resonance is an Antikaon-Nucleon Molecule

Jonathan M. M. Hall,[1] Waseem Kamleh,[1] Derek B. Leinweber,[1] Benjamin J. Menadue,[1,2] Benjamin J. Owen,[1] Anthony W. Thomas,[1,3] and Ross D. Young[1,3]

[1]*Special Research Centre for the Subatomic Structure of Matter (CSSM), Department of Physics, University of Adelaide, Adelaide, South Australia 5005, Australia*
[2]*National Computational Infrastructure (NCI), Australian National University, Canberra, Australian Capital Territory 0200, Australia*
[3]*ARC Centre of Excellence for Particle Physics at the Terascale (CoEPP), Department of Physics, University of Adelaide, Adelaide, South Australia 5005, Australia*

For almost 50 years the structure of the $\Lambda(1405)$ resonance has been a mystery. Even though it contains a heavy strange quark and has odd parity, its mass is lower than any other excited spin-1/2 baryon. Dalitz and co-workers speculated that it might be a molecular state of an antikaon bound to a nucleon. However, a standard quark-model structure is also admissible. Although the intervening years have seen considerable effort, there has been no convincing resolution. Here we present a new lattice QCD simulation showing that the strange magnetic form factor of the $\Lambda(1405)$ vanishes, signaling the formation of an antikaon-nucleon molecule. Together with a Hamiltonian effective-field-theory model analysis of the lattice QCD energy levels, this strongly suggests that the structure is dominated by a bound antikaon-nucleon component. This result clarifies that not all states occurring in nature can be described within a simple quark model framework and points to the existence of exotic molecular meson-nucleon bound states.

arXiv:1411.3402v2 [hep-lat] 14 Apr 2015

The spectrum of hadronic excitations observed at accelerator facilities around the world manifests the fundamental interactions of elementary quarks and gluons, governed by the quantum field theory of quantum chromodynamics (QCD). Understanding the complex emergent phenomena of this field theory has captivated the attention of theoretical physicists for more than four decades.

Of particular interest is the unusual nature of the lowest-lying excitation of the Lambda baryon [1–8] the "Lambda 1405," $\Lambda(1405)$. The Lambda baryon is a neutral particle, like the neutron, composed of the familiar up (u) and down (d) quarks together with a strange quark (s).

For almost 50 years the structure of the $\Lambda(1405)$ resonance has been a mystery. Even though it contains a relatively massive strange quark and has odd parity, *both of which should increase its mass*, it is, in fact, lighter than any other excited spin-1/2 baryon. Identifying the explanation for this observation has challenged theorists since its discovery in the 1960s through kaon-proton [1] and pion-proton production [2] experiments.

While the quantum numbers of the $\Lambda(1405)$ can be described by three quarks, (uds), its totally unexpected position in the spectrum has rendered its structure quite mysterious [9]. Before the quark model had been established, Dalitz and co-workers [10, 11] speculated that it might be a molecular state of an antikaon, $\overline{K}$, bound to a nucleon, N. Whereas the $\pi\Sigma$ energy threshold is well below the $\Lambda(1405)$ resonance position the $\overline{K}N$ energy threshold is only slightly above. A molecular $\overline{K}N$ bound state with a small amount of binding energy presents an interesting candidate for the structure of the $\Lambda(1405)$. Although the intervening years have seen enormous effort devoted to this resonance [8–24], there has been no convincing resolution.

Herein, we present the very first lattice QCD calculation of the electromagnetic form factors of the $\Lambda(1405)$. This calculation reveals the vanishing of the strange quark contribution to the magnetic form factor of the $\Lambda(1405)$ in the regime where the masses of the up and down quarks approach their physical values. This result is very naturally explained if the state becomes a molecular $\overline{K}N$ bound state in that limit. When this observation is combined with a Hamiltonian effective-field-theory analysis of the structure of the state as a function of its light quark mass, which shows $\overline{K}N$ dominance and a rapidly decreasing wave function renormalization constant in the same limit, it constitutes strong evidence that the $\Lambda(1405)$ is a bound $\overline{K}N$ molecule.

Our calculations are based on the $32^3\times64$ full-QCD ensembles created by the PACS-CS collaboration [25], made available through the International Lattice Data Grid (ILDG) [26]. These ensembles provide a lattice volume of $(2.90\text{ fm})^3$ with five different masses for the light u and d quarks and constant strange-quark simulation parameters. We simulate the valence strange quark with a hopping parameter (governing the strange quark mass) of $\kappa_s = 0.13665$. This value reproduces the correct kaon mass in the physical limit [27]. We use the squared pion mass as a renormalization group invariant measure of the quark mass. The lightest PACS-CS ensemble provides a pion mass of 156 MeV, only slightly above the physical value of 140 MeV realized in nature.

To study the $\Lambda(1405)$ energy, one acts on the QCD vacuum with baryon interpolating fields defining specific spin, flavor, color and parity symmetries for the quark field operators. We consider local three-quark operators providing both scalar and vector diquark spin configurations for the quarks [28]. As the $\Lambda(1405)$ has the valence quark assignment of (uds), it has overlap with both octet and singlet flavor symmetries. The flavor symmetry is exact when all three quarks have the same mass and electromagnetic charges are neglected. However, the strange quark mass is much larger than the u and d quark masses, and one expects that the eigenstates of QCD should

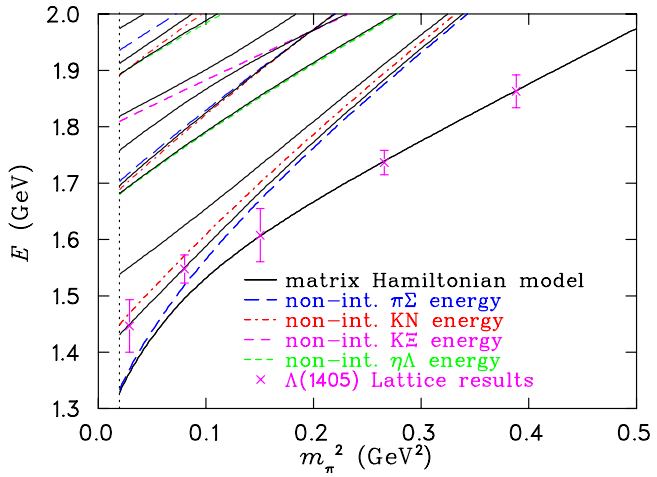

FIG. 1. The quark-mass dependence ($m_q \propto m_\pi^2$) of the lowest-lying $\Lambda(1405)$ states observed in our lattice QCD calculations is illustrated by the discrete points at each of the pion masses available in the PACS-CS ensembles. The low-lying energy spectrum of our Hamiltonian model (solid curves) constrained to the lattice QCD results (discrete points) is also illustrated. The associated noninteracting meson-baryon basis states are illustrated by the dashed curves and the vertical dashed line indicates the physical pion mass.

involve a superposition of octet and singlet symmetries.

The mixing of spin-flavor symmetries in the QCD eigenstates demands a linear superposition of these interpolators when creating an eigenstate of QCD. The correlation matrix approach [29, 30] provides an effective means for determining this superposition via generalized eigenvalue equations.

The basis and superposition of three-quark interpolating fields successfully isolating the $\Lambda(1405)$ were determined in Ref. [28] and are used in the present study of the quark-sector contributions to the electromagnetic form factors of the $\Lambda(1405)$. The superposition is illustrated in Fig. 1 of Ref. [31] and is characterized by a dominant flavor-singlet component with the flavor-octet vector-diquark interpolator gaining importance as the u and d quarks become light and $SU(3)$ flavor symmetry is broken. Narrow and wide gauge-invariant Gaussian-smeared quark sources are considered with the narrow smearing diminishing in importance as the u and d quarks become light.

The success of this approach in accurately isolating the $\Lambda(1405)$, even at the lightest quark mass considered, is illustrated by the long Euclidean-time single-state stability of the $\Lambda(1405)$ two-point correlation function presented in Fig. 2 of Ref. [31]. We note this is realized without resort to two-particle interpolators. This discovery of a low-lying $\Lambda(1405)$ mass [28] has since been confirmed independently [32].

The quark-mass dependence of the lowest-lying state observed in our lattice QCD calculations is illustrated in Fig. 1 by the discrete points at each of the pion masses available in the PACS-CS simulations. The scale is set via the Sommer parameter [33] with $r_0 = 0.492$ fm [25]. This low-lying state is predominantly flavor-singlet, with an important contribution from octet interpolators emerging as one moves away from the $SU(3)$ flavor-symmetric limit [28].

The connection of these lattice QCD results obtained on a finite volume lattice to the infinite volume limit of nature is made through a matrix Hamiltonian model which describes the composition of the lattice QCD eigenstates in terms of effective meson-baryon degrees of freedom. The noninteracting meson-baryon basis states and the results of the model are illustrated in Fig. 1 and will be discussed in further detail below.

The isolation of an individual energy eigenstate enables the investigation of other properties of the $\Lambda(1405)$ on the finite volume lattice. The electromagnetic form factors are particularly interesting as they provide insight into the distribution of charge and magnetism within the $\Lambda(1405)$. Moreover, the form factors can be resolved one quark flavor at a time.

The strange quark magnetic form factor of the $\Lambda(1405)$ is crucial to the present analysis because it provides direct insight into the possible dominance of a molecular $\overline{K}N$ bound state. In forming such a molecular state, the $\Lambda(uds)$ valence quark configuration is complemented by a $u\overline{u}$ quark–anti-quark pair making a $K^-(s\overline{u})$ proton (uud) bound state, or a $d\overline{d}$ quark–anti-quark pair making a $\overline{K}^0(s\overline{d})$ neutron (ddu) bound state. In both cases the strange quark is confined within a spin-0 kaon and has no preferred spin orientation. Because of this and the fact that the antikaon has zero orbital angular momentum in order to conserve parity, the strange quark *cannot* contribute to the magnetic form factor of the $\Lambda(1405)$. On the other hand, if the $\Lambda(1405)$ were a $\pi\Sigma$ state or an elementary three-quark state the strange quark must make a sizable contribution to the magnetic form factor. In summary, only if the $\overline{K}N$ component in the structure of the $\Lambda(1405)$ is dominant would one expect to find a vanishing strange quark magnetic form factor.

Techniques for calculating the Sachs electromagnetic form factors of spin-1/2 baryons in lattice QCD were established in Ref. [34]. A fixed boundary condition is applied in the time direction at $t = 0$ and the fermion sources are placed at $t = 16$. States are evolved in Euclidean time to $t = 21$ where an $\mathcal{O}(a)$-improved conserved vector current [35, 36] is inserted with three momentum $\vec{q} = (2\pi/L, 0, 0)$ providing $Q^2 = 0.16(1)$ GeV$^2/c^2$.

To measure the electromagnetic properties of the $\Lambda(1405)$ in lattice QCD, one probes the state with the conserved vector current at a time well separated from the creation and annihilation points to ensure single-state isolation. By taking the ratio of this three-point correlation function with the two-point correlation function from the mass analysis, we create a direct measure of the Sachs electric and magnetic form factors.

Figure 2 presents the Euclidean time dependence of this measure for the strange quark contribution to the Sachs magnetic form factor, $\mathcal{G}_M^s$, of the $\Lambda(1405)$ at $Q^2 \simeq 0.16$ GeV$^2/c^2$. Results for two different ensembles are presented. As is standard for quark-sector contributions, the electric charge factor for the quark charge has not been included; *i.e.* the result is for a single quark of unit charge. The best fit plateaus, as identified by a covariance matrix based χ^2 analysis, are also illustrated. The rapid onset of the plateau following the electromagnetic current at $t = 21$ reflects our use of optimized

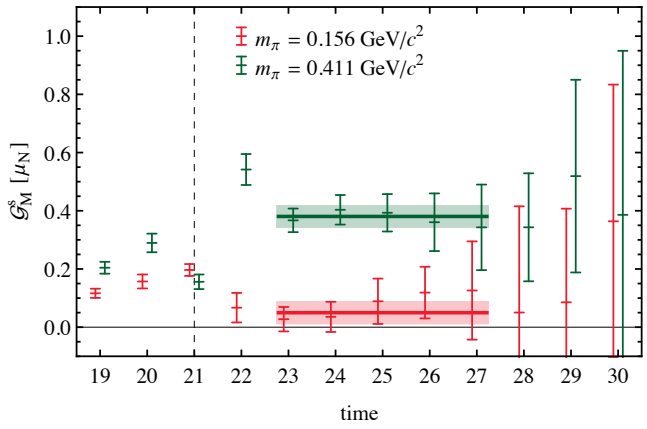

FIG. 2. Ratio of three- and two-point functions providing the strange-quark contribution to the Sachs magnetic form factor of the $\Lambda(1405)$. Results at two different pion masses describing the light u and d quark masses are illustrated for $Q^2 \simeq 0.16$ GeV$^2/c^2$. The vertical dashed line indicates the introduction of the electromagnetic current at $t = 21$ following the baryon source at $t = 16$.

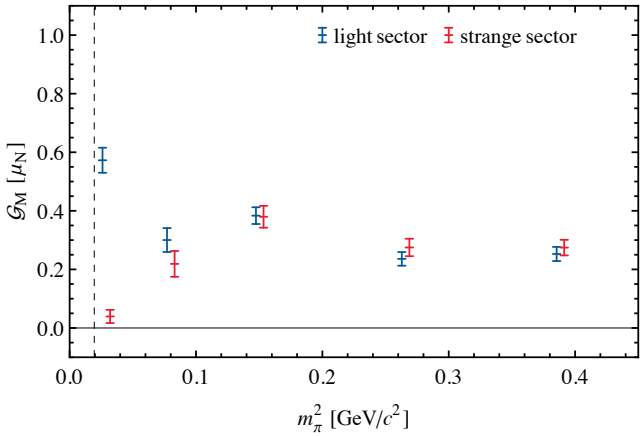

FIG. 3. The light (u or d) and strange (s) quark contributions to the magnetic form factor of the $\Lambda(1405)$ at $Q^2 \simeq 0.16$ GeV$^2/c^2$ are presented as a function of the light u and d quark masses, indicated by the squared pion mass, m_π^2. Sector contributions are for single quarks of unit charge. The vertical dashed line indicates the physical pion mass.

interpolating fields.

Figure 3 presents ${\mathcal{G}_M}^s$ for the $\Lambda(1405)$ at $Q^2 \simeq 0.16$ GeV$^2/c^2$ for all five ensembles available from PACS-CS. Variation of the light u and d quark masses is indicated by the squared pion mass, m_π^2. At the heaviest u and d quark masses approaching the $SU(3)$ flavor limit, $m_u = m_d = m_s$, the underlying approximate flavor-singlet structure is manifest in ${\mathcal{G}_M}^s$ with the light and strange sectors contributing equally. Similar results were observed for the electric form factors of the $\Lambda(1405)$ [31]. Even though the light-quark sector is becoming much lighter, this symmetry persists well towards the physical point. Only by directly simulating QCD in the realm of quark masses realized in nature can the vanishing of the strange quark contribution be revealed.

At the lightest quark-mass ensemble closest to nature, the strange quark contribution to the magnetic form factor of the $\Lambda(1405)$ drops by an order of magnitude and approaches zero. As the simulation parameters describing the strange quark are held fixed, this is a remarkable environmental effect of unprecedented strength. As the u and d quark masses become light, and the cost of creating $u\overline{u}$ and $d\overline{d}$ quark-antiquark pairs from the QCD vacuum diminishes, we observe an important rearrangement of the quark structure within the $\Lambda(1405)$ consistent with the dominance of a molecular $\overline{K}N$ bound state.

To connect these results obtained for a QCD eigenstate on the finite volume of the lattice to the infinite volume baryon resonance of nature, we construct a finite-volume Hamiltonian model using a basis of single- and two-particle noninteracting meson-baryon states available on the finite-volume periodic lattice. We follow the approach established in Ref. [37] where the eigenvalue equation of the model is designed to reproduce finite-volume chiral effective field theory [38–41] in the weak coupling limit. Finite-volume models [17, 37, 42] are particularly useful in interpreting the composition of the energy spectrum observed in lattice QCD results.

In constructing the Hamiltonian, the four octet meson-baryon interaction channels of the $\Lambda(1405)$ are included: $\pi\Sigma$, $\overline{K}N$, $K\Xi$ and $\eta\Lambda$. The matrix representation of the Hamiltonian contains diagonal entries corresponding to the relativistic noninteracting meson-baryon energies available on the finite periodic volume at total three-momentum zero. It also includes a single-particle state with a bare mass parameter, m_0. To access quark masses away from the physical point, the mass of the bare three-quark state is allowed to grow linearly with the quark mass (or pion mass squared), $m_0 + \alpha_0\, m_\pi^2$. The two parameters of the Hamiltonian model, the bare mass, m_0, and the rate of growth, α_0, are constrained [43] by the lattice QCD results.

The interaction entries describe the coupling of the single-particle state to the two-particle meson-baryon states [44–46]. The strength of the interaction is selected to reproduce the physical decay width (to $\pi\Sigma$) of 50 ± 2 MeV [47] for the $\Lambda(1405)$ in the infinite-volume limit. The couplings for other channels are related by $SU(3)$-flavor symmetry [12–14].

In solving the Hamiltonian model, one naturally obtains important nonperturbative avoided level crossings in the quark mass and volume dependence of the eigenstates, vital to describing the lattice QCD results. The solid curves of Fig. 1 illustrate the best fit of the Hamiltonian model to the lattice QCD results.

The three heaviest quark masses considered on the lattice correspond to a stable odd-parity $\Lambda(1405)$, as the $\pi\Sigma$ threshold energy exceeds that of the $\Lambda(1405)$. However, as the physical pion mass is approached, the $\pi\Sigma$ threshold energy decreases and a nontrivial mixing of states associated with an avoided level crossing of the transitioning $\pi\Sigma$ threshold occurs. At the lightest two quark masses considered, the $\Lambda(1405)$ corresponds to the second state of the Hamiltonian model with a $\pi\Sigma$-dominated eigenstate occupying the lowest energy position.

The eigenvectors of the Hamiltonian system provide the overlap of the basis states with the eigenstates and thus de-

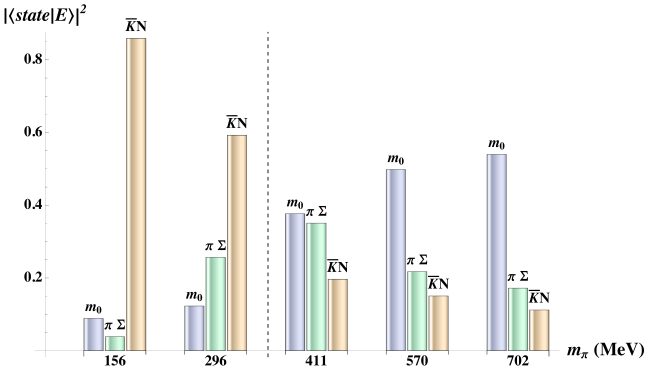

FIG. 4. The overlap of the basis state, $|state\rangle$, with the energy eigenstate $|E\rangle$ for the $\Lambda(1405)$, illustrating the composition of the $\Lambda(1405)$ as a function of pion mass. Basis states include the single particle state, denoted by m_0, and the two-particle states $\pi\Sigma$ and $\overline{K}N$. A sum over all two-particle momentum states is done in reporting the probability for the two-particle channels. Pion masses are indicated on the x axis with the vertical dashed line separating the first state for the heaviest three masses from the second state for the lightest two masses.

scribe the underlying composition of the eigenstates. As the first and second eigenstates are dominated by the single-particle state and the two-particle channels $\pi\Sigma$ and $\overline{K}N$, we illustrate these in Fig. 4 for each value of pion mass considered in the lattice QCD simulations. A sum over all two-particle momentum states is done in reporting the probability of the two-particle channels.

At the lightest pion mass, $m_\pi = 156$ MeV, the Hamiltonian model eigenstate for the $\Lambda(1405)$ is dominated by the $\overline{K}N$ channel in complete agreement with the explanation of the observed, vanishing strange quark contribution to the magnetic form factor. A small but nontrivial role for the single-particle three-quark state enables the excitation of this state in the lattice correlation matrix analysis of three-quark operators. In contrast, the lowest-lying eigenstate of the Hamiltonian model at $m_\pi = 156$ MeV is dominated by $\pi\Sigma$, with very small single-particle content, which explains why it is missing from the lattice QCD spectrum.

Having confirmed that the $\Lambda(1405)$ state observed on the lattice is best described as a molecular $\overline{K}N$ bound state, it remains to demonstrate the connection between the finite-volume lattice eigenstates and the infinite-volume resonance found in nature. The quark-mass behaviour of the $\Lambda(1405)$ energy in the infinite-volume limit can be reconstructed from the finite-volume Hamiltonian model by considering the principal-value continuum versions of the loop integral contributions from all channels. A bootstrap error analysis provides a resonance energy of $1.48^{+0.17}_{-0.07}$ GeV. The distribution of the bootstrap analysis is sharply peaked around the most probable value of 1.41 GeV in good agreement with experiment. Further details may be found in Ref. [48].

In summary, the $\Lambda(1405)$ has been identified in first-principles lattice QCD calculations through a study of its quark mass dependence and its relation to avoided level crossings in finite-volume effective field theory. The structure of the $\Lambda(1405)$ is dominated by a molecular bound state of an antikaon and a nucleon. This structure is signified both by the vanishing of the strange quark contribution to the magnetic moment of the $\Lambda(1405)$ and by the dominance of the $\overline{K}N$ component found in the finite-volume effective field theory Hamiltonian treatment.

At the same time, the presence of a nontrivial single-particle three-quark component explains why the state is readily accessible in lattice correlation matrix analyses constructed with three-quark operators. In the infinite-volume limit, the Hamiltonian model describes a quark mass dependence that is consistent with nature.

Acknowledgements: We thank PACS-CS Collaboration for making their gauge configurations available and acknowledge the important ongoing support of the ILDG. This research was undertaken with the assistance of resources awarded at the NCI National Facility in Canberra, Australia, and the iVEC facilities at Murdoch University (iVEC@Murdoch) and the University of Western Australia (iVEC@UWA). These resources are provided through the National Computational Merit Allocation Scheme and the University of Adelaide Partner Share supported by the Australian Government. We also acknowledge eResearch SA for their support of our supercomputers. This research is supported by the Australian Research Council through the ARC Centre of Excellence for Particle Physics at the Terascale, and through Grants No. DP120104627 (D.B.L.), No. DP140103067 (D.B.L. and R.D.Y.), No. FT120100821 (R.D.Y.) and No. FL0992247 (A.W.T.).

[1] M. H. Alston, L. W. Alvarez, P. Eberhard, M. L. Good, W. Graziano, *et al.*, Phys.Rev.Lett. **6**, 698 (1961).
[2] A. Engler, H. Fisk, R. Kraemer, C. Meltzer, J. Westgard, *et al.*, Phys. Rev. Lett. **15**, 224 (1965).
[3] R. Hemingway, Nucl.Phys. **B253**, 742 (1985).
[4] B. Riley, I. Wang, J. Fetkovich, and J. Mckenzie, Phys.Rev. **D11**, 3065 (1975).
[5] J. Esmaili, Y. Akaishi, and T. Yamazaki, Phys.Lett. **B686**, 23 (2010), arXiv:0906.0505 [nucl-th].
[6] G. Agakishiev *et al.* (HADES Collaboration), Phys.Rev. **C87**, 025201 (2013), arXiv:1208.0205 [nucl-ex].
[7] K. Olive *et al.* (Particle Data Group), Chin.Phys. **C38**, 090001 (2014).
[8] M. Hassanvand, S. Z. Kalantari, Y. Akaishi, and T. Yamazaki, Phys.Rev. **C87**, 055202 (2013), arXiv:1210.7725 [nucl-th].
[9] F. Close and R. Dalitz, OXFORD-TP-73-80, C80-03-24.2-5 (1980).
[10] R. Dalitz and S. Tuan, Annals Phys. **10**, 307 (1960).
[11] R. Dalitz, T. Wong, and G. Rajasekaran, Phys. Rev. **153**, 1617 (1967).
[12] E. Veit, B. K. Jennings, R. Barrett, and A. W. Thomas, Phys. Lett. **B137**, 415 (1984).
[13] E. Veit, B. K. Jennings, A. W. Thomas, and R. Barrett, Phys. Rev. **D31**, 1033 (1985).
[14] N. Kaiser, P. Siegel, and W. Weise, Nucl. Phys. **A594**, 325 (1995), arXiv:nucl-th/9505043 [nucl-th].

[15] M. Lage, U.-G. Meissner, and A. Rusetsky, Phys. Lett. **B681**, 439 (2009), arXiv:0905.0069 [hep-lat].

[16] D. Jido, T. Sekihara, Y. Ikeda, T. Hyodo, Y. Kanada-En'yo, *et al.*, Nucl. Phys. **A835**, 59 (2010), arXiv:1003.4560 [nucl-th].

[17] M. Doring, U. Meißner, E. Oset, and A. Rusetsky, Eur. Phys. J. **A48**, 114 (2012), arXiv:1205.4838 [hep-lat].

[18] M. Mai and U.-G. Meissner, Nucl. Phys. **A900**, 51 (2013), arXiv:1202.2030 [nucl-th].

[19] K. Miyagawa and J. Haidenbauer, Phys. Rev. **C85**, 065201 (2012), arXiv:1202.4272 [nucl-th].

[20] A. Martinez Torres, M. Bayar, D. Jido, and E. Oset, Phys. Rev. **C86**, 055201 (2012), arXiv:1202.4297 [hep-lat].

[21] L. Roca and E. Oset, Phys. Rev. **C87**, 055201 (2013), arXiv:1301.5741 [nucl-th].

[22] T. Sekihara and S. Kumano, Phys. Rev. **C89**, 025202 (2014), arXiv:1311.4637 [nucl-th].

[23] J.-J. Xie, B.-C. Liu, and C.-S. An, Phys. Rev. **C88**, 015203 (2013), arXiv:1307.3707 [nucl-th].

[24] J. Oller, Int. J. Mod. Phys. Conf. Ser. **26**, 1460096 (2014), arXiv:1309.2196 [nucl-th].

[25] S. Aoki *et al.* (PACS-CS Collaboration), Phys. Rev. **D79**, 034503 (2009), arXiv:0807.1661 [hep-lat].

[26] M. G. Beckett, B. Joo, C. M. Maynard, D. Pleiter, O. Tatebe, *et al.*, Comput. Phys. Commun. **182**, 1208 (2011), arXiv:0910.1692 [hep-lat].

[27] B. J. Menadue, W. Kamleh, D. B. Leinweber, M. S. Mahbub, and B. J. Owen, PoS **LATTICE2012**, 178 (2012).

[28] B. J. Menadue, W. Kamleh, D. B. Leinweber, and M. S. Mahbub, Phys. Rev. Lett. **108**, 112001 (2012), arXiv:1109.6716 [hep-lat].

[29] C. Michael, Nucl. Phys. **B259**, 58 (1985).

[30] M. Luscher and U. Wolff, Nucl. Phys. **B339**, 222 (1990).

[31] B. J. Menadue, W. Kamleh, D. B. Leinweber, M. S. Mahbub, and B. J. Owen, PoS **LATTICE2013**, 280 (2013), arXiv:1311.5026 [hep-lat].

[32] G. P. Engel, C. Lang, and A. Schafer, Phys. Rev. **D87**, 034502 (2013), arXiv:1212.2032 [hep-lat].

[33] R. Sommer, Nucl. Phys. **B411**, 839 (1994), arXiv:hep-lat/9310022 [hep-lat].

[34] D. B. Leinweber, R. Woloshyn, and T. Draper, Phys. Rev. **D43**, 1659 (1991).

[35] G. Martinelli, C. T. Sachrajda, and A. Vladikas, Nucl. Phys. **B358**, 212 (1991).

[36] S. Boinepalli, D. Leinweber, A. Williams, J. Zanotti, and J. Zhang, Phys. Rev. **D74**, 093005 (2006), arXiv:hep-lat/0604022 [hep-lat].

[37] J. Hall, A. C. P. Hsu, D. Leinweber, A. Thomas, and R. Young, Phys. Rev. **D87**, 094510 (2013), arXiv:1303.4157 [hep-lat].

[38] M. J. Savage, Phys. Lett. **B331**, 411 (1994), arXiv:hep-ph/9404285 [hep-ph].

[39] C. Garcia-Recio, J. Nieves, E. Ruiz Arriola, and M. Vicente Vacas, Phys. Rev. **D67**, 076009 (2003), arXiv:hep-ph/0210311 [hep-ph].

[40] T. Sekihara, T. Hyodo, and D. Jido, Phys. Rev. **C83**, 055202 (2011), arXiv:1012.3232 [nucl-th].

[41] T. Hyodo and D. Jido, Prog. Part. Nucl. Phys. **67**, 55 (2012), arXiv:1104.4474 [nucl-th].

[42] J.-J. Wu, T.-S. Lee, A. Thomas, and R. Young, Phys.Rev. **C90**, 055206 (2014), arXiv:1402.4868 [hep-lat].

[43] M. Powell, The Computer Journal **7**, 155 (1964).

[44] D. B. Leinweber, A. W. Thomas, and R. D. Young, Phys. Rev. Lett. **92**, 242002 (2004), arXiv:hep-lat/0302020 [hep-lat].

[45] R. Young and A. Thomas, Phys. Rev. **D81**, 014503 (2010), arXiv:0901.3310 [hep-lat].

[46] S. Beane, E. Chang, W. Detmold, H. Lin, T. Luu, *et al.*, Phys. Rev. **D84**, 014507 (2011), arXiv:1104.4101 [hep-lat].

[47] J. Beringer *et al.* (Particle Data Group), Phys. Rev. **D86**, 010001 (2012).

[48] J. M. M. Hall, W. Kamleh, D. B. Leinweber, B. J. Menadue, B. J. Owen, A. W. Thomas, and R. D. Young, PoS **LATTICE2014**, 094 (2014), arXiv:1411.3781 [hep-lat].